Assessing future exploration potential of the Cobar District using integrated 3D geological modelling and geophysical inversion.

SPAMPINATO, G.[1]   **Austin, J. R.**[1]

[1]*Mineral Exploration Cooperative Research Centre, CSIRO, Linfield, Australia*
giovanni.spampinato@csiro.au   james.austin@csiro.au

SUMMARY

The late Silurian to early Devonian Cobar Supergroup hosts a variety of polymetallic mineral systems, forming the most mineralised sedimentary sequence within the Palaeozoic Lachlan Orogen. However, several areas undercover are still unmapped, posing a serious impediment to the discovery of new resources.

3D geological modelling has become a fundamental tool for understanding the architecture and unravelling the mineral potential of buried terranes. 3D modelling and geophysical inversion was undertaken in key areas of the central and southern Cobar Basin in order to identify connections between the broad scale architecture and the localisation of mineral deposits and provide an updated framework for future exploration.

Datasets used in the construction of 3D geological and structural models include surface geological mapping, geological cross-sections, well data, digital elevation models, airborne electromagnetic surveys, gravity and magnetic data.

Geophysical inversion was performed using the VOXI magnetic vector inversion (MVI), which solves the 3D inverse problem using unconstrained magnetisation vectors (attempting to account for induced magnetisation, remanence, anisotropy and self- demagnetisation mathematically). The unconstrained VOXI MVI not only highlighted source bodies reflecting the CSA, Peak Gold and Nymagee deposits, but also identified prospective rocks within the Cobar mineral system that are underexplored.

Regional scale magnetics shows that the Cobar-type deposits are controlled by major N-S-trending faults at the regional scale, whereas 3D EM inversions suggest that mineralisation is localised by NE- and NW-trending lateral faults at the camp scale. VOXI MVI results also suggest that remanent magnetization accounts for a component of the magnetic signature of these deposits and ignoring remanent magnetization could prove a costly mistake in targeting Cobar type systems.

The outputs of this research provide new insights for undercover extension of known mineralisation within the Cobar Basin and will assist in future exploration.

Key words: Cobar Basin, 3D Modelling, Geophysical Inversion, Magnetics, Mineral Exploration, Remanence.

INTRODUCTION

The late Silurian to early Devonian Cobar Basin in New South Wales is the most mineralised Palaeozoic sedimentary basin in the Lachlan Orogen, hosting massive sulphides, clastic hosted Pb-Zn mineralisation and epithermal gold (David, 2018; Fitzherbert, 2020; Glen, 1991). However, prospective areas undercover remain underexplored and known metal occurrences occur predominantly where the prospective rocks are at or near-surface.

3D geological modelling and 3D quantitative interpretation of geophysical data have become a crucial tool to visualise and analyse stratigraphic contacts, fault and fold geometries, rock volumes and spatial changes in physical or mineralogical properties of lithological units (Betts et al., 2004; Spampinato et al., 2015a, 2015b; Williams et al., 2010, Witter et al., 2016).

In this study, we perform unconstrained geophysical inversion of magnetic data to identify magnetized prospective rocks within the Cobar mineral system. The results of this study inform the relationship between prospective areas and major structures that controlled the architecture of the region and provides insights for the investigation of the undercover extensions of the known mineralised parts of the Cobar Basin.

This study is part of the Mineral Exploration Cooperative Research Centre (MinEx CRC) Program and focus on National Drilling Initiative's (NDI) case study areas in NSW (Figure 1). MinEx CRC is a 10-year program which brings together industry partners, government agencies, research organizations and universities to improve the understanding of Australia's geology, mineral deposits and groundwater resources in covered terrains and develop new tools to reduce exploration risk, supply pre-competitive geoscientific data and encourage mineral exploration in prospective areas undercover (Folkes et al., 2022).
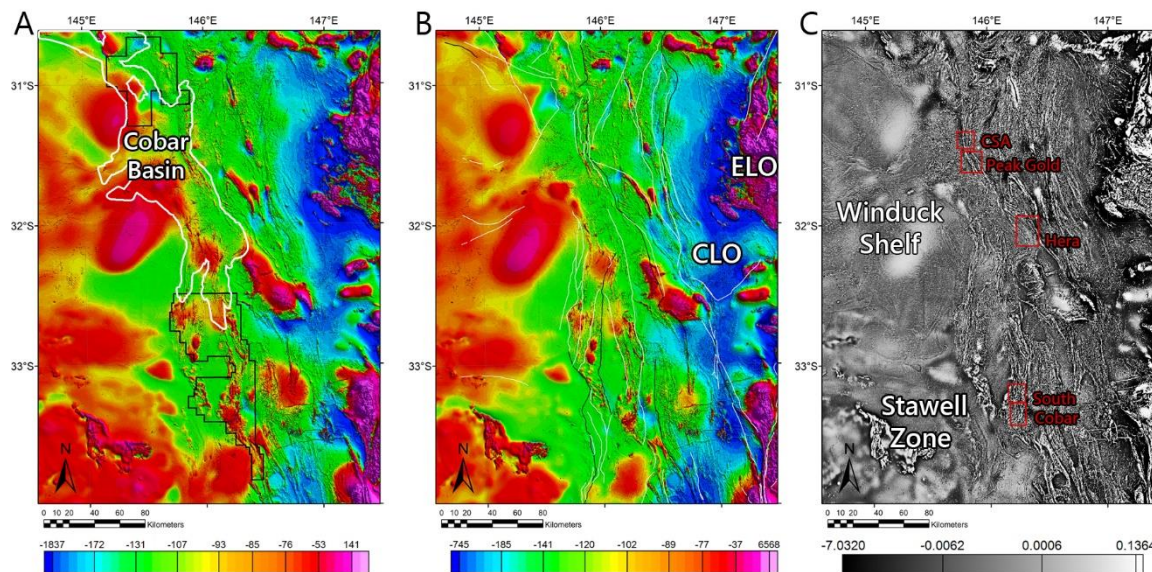
Figure 1. Pseudo-colour image of the TMI (A), RTP (B) and greyscale image of the 1VD (C) of aeromagnetic anomalies of the Cobar Basin and surrounding regions. Black polygons are the location of the Minex CRC NDI areas, white and black line are major faults and red rectangles are the location of the geophysically inverted models. CLO= central Lachlan Orogen; ELO= eastern Lachlan Orogen.

METHODOLOGY

Constraining geological and geophysical data were imported into SKUA-GOCAD™ to produce an initial 3D lithological and structural model of the areas of interest (example in Figure 2). SKUA-GOCAD™ and the GOCAD Mining Suite™ form an advanced geoscience software platform used to build and analyse quantitative, multi-disciplinary 3D Earth models (Aillères, 2000; Witter, 2015). The top surface of the starting 3D models is represented by the DEM. The top of magnetization horizon is represented by the top of fresh Pre-Carboniferous basement units. Basement architecture, major faults and strike-slip structures have been reviewed and modelled using the interpretation from AEM data (Folkes et al., 2022; Spampinato, 2022; this study), magnetic and gravity data and the fault attribution from the Seamless Geology Dataset (Colquhoun et al., 2020).
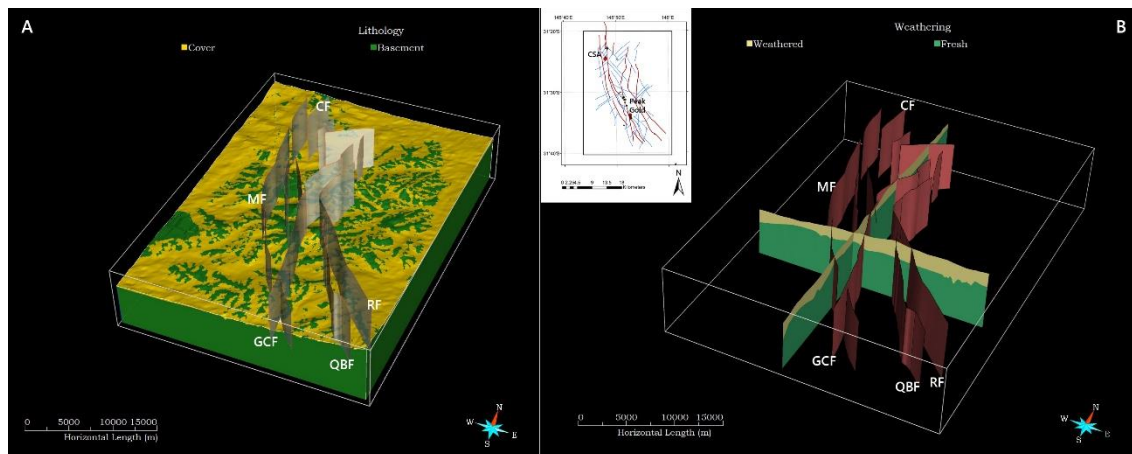

Figure 2. A) Basement Elevation 3D Model across the CSA and Peak Gold mines region showing surface topography, outcropping pre-Carboniferous basement units and location of major faults. B) NS and EW oriented cross-sections extracted from CSA and Peak Gold mines region 3D Model. The transported cover, saprolitic horizon and weathered rocks have been grouped into one horizon, termed 'weathered'. On the top, plan figure showing the location of the 3D model, major faults (red lines) minor faults (blue lines) and constraining drillholes (green dots). CF= Cobar Fault; MF= Myrt Fault; RF= Roockery fault; GCF= Great Chesney Fault; QBF= Queen Bee Fault. The 3D model has a 10X times vertical exaggeration.

The starting model is discretised into a mesh volume which forms the input file for the inversion process. Each cell forming the mesh is assigned an initial petrophysical (for example magnetic susceptibility) or lithological (unit, formation) property. Cell property (in a property inversion) or shape (in a geometrical inversion) can vary during the inversion process. At each iteration, the geophysical response of the geologic model is calculated and compared to the

observed data. The model parameters are adjusted at each iteration to minimise the misfit between the observed and calculated data. The calculated magnetic signal is the vector summation of all contributing cells.

Unconstrained geophysical inversion involves computation of a best fit model purely based on mathematical constraints. This computational process creates a model that satisfies the geophysical dataset alone (Fullagar and Pears, 2013). For this project, the main inversion tool was Geosoft VOXI™ Earth Modelling Extension. Geosoft VOXI™ is a cloud-based geophysical inversion modelling tool. The software can generate geologically constrained and unconstrained 3D inversions and forward models of gravity and magnetic data and can account for induced magnetisation and remanence. Inversion has been performed using Geosoft VOXI™ magnetic vector inversion (VOXI MVI) and VOXI™ purely induced inversion (VOXI SUS).

Geophysically inverted models have been created for the CSA and Peak Gold mines region, Nymagee and Hera mines region and the south Cobar District, respectively (Figure 1). Regional trend removal has been undertaken to remove the effect of the regional signal coming from source deeper than the bottom of the model. Upon data review, a model mesh of 100m x 100 m x 40 m was considered a suitable resolution.

<div align="center">

OBSERVATIONS AND RESULTS

</div>

CSA Mine Region Inverted 3D Model

The CSA Mine deposit sits on a sub-circular positive magnetic anomaly, superimposed on a N-S- to NNW-trending magnetic ridge (Figure 3). Within the CSA Mine Region Inverted 3D Model, VOXI MVI indicates that the host rock has a calculated magnetic susceptibility <0.0005 SI. VOXI SUS shows background susceptibility values below 0.0002 SI (Figure 4).

The 3D geophysical inversion generated relatively highly magnetized rocks with susceptibility values up to 0.18 SI for VOXI MVI and 0.15 SI for VOXI SUS, respectively (Figure 4). Shallow, magnetized rocks with a minimum susceptibility value of 0.005 SI are located at the intersection of major NNW-trending structures and NE-trending tear faults, in a highly deformed region (Figure 5). However, the magnetized source bodies generated by VOXI MVI are considerably thinner (up to 741m thick) when compared to the magnetic domains generated by VOXI SUS (Figure 5).

Within the VOXI MVI inverted model, the CSA deposit is comprised in a weakly to moderately magnetic domain with calculated susceptibility values ranging between 0.0005 SI and 0.1 SI. VOXI SUS was able to generate a distinct weakly to moderate magnetic domain with calculated susceptibility values ranging between 0.003 SI and 0.02 SI that correlates with the central and northern CSA Mine deposit.
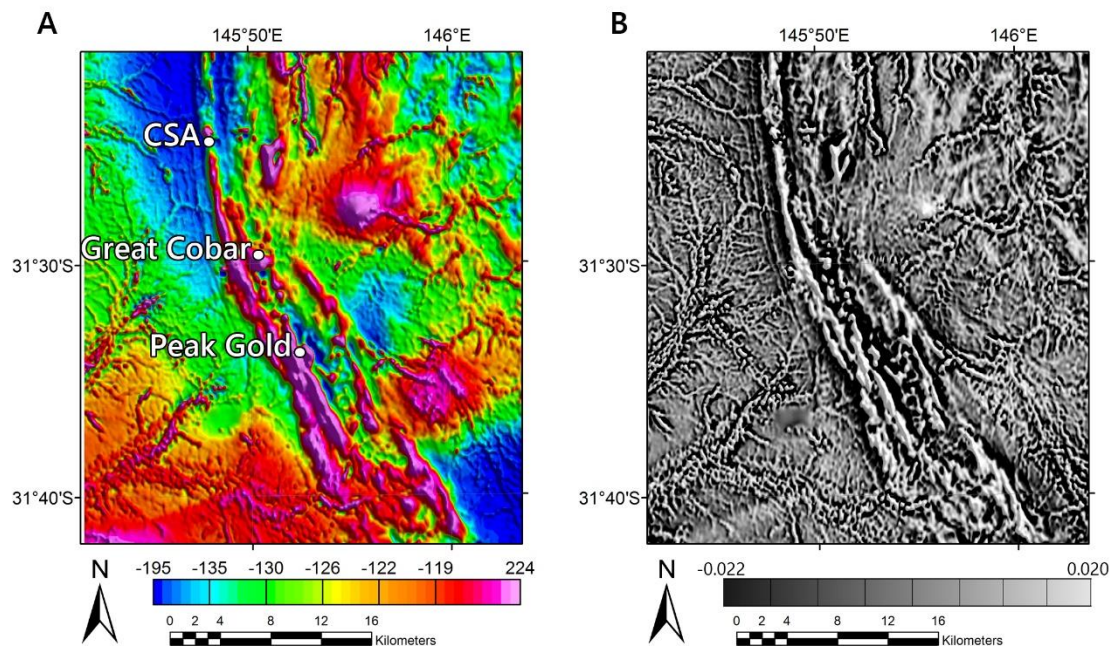

Figure 3. Pseudo-colour image of the RTP (A) and 1VD (B) of aeromagnetic anomalies over the CSA and Peak Gold mines region.
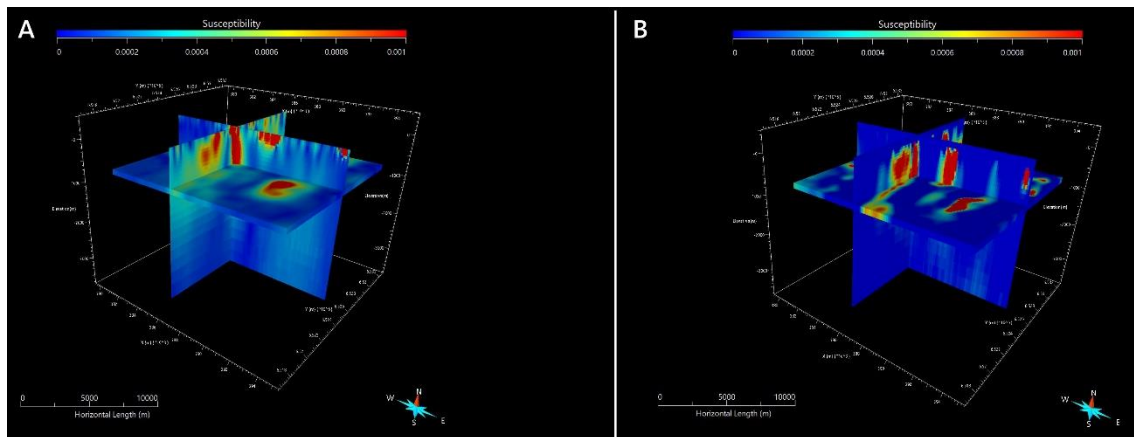
Figure 4. Results from VOXI MVI (A) and VOXI SUS (B) for the CSA Mine region. Magnetic susceptibilities are in SI. The image has a 3X times vertical exaggeration. The location of the inverted model is shown in Figure 1.
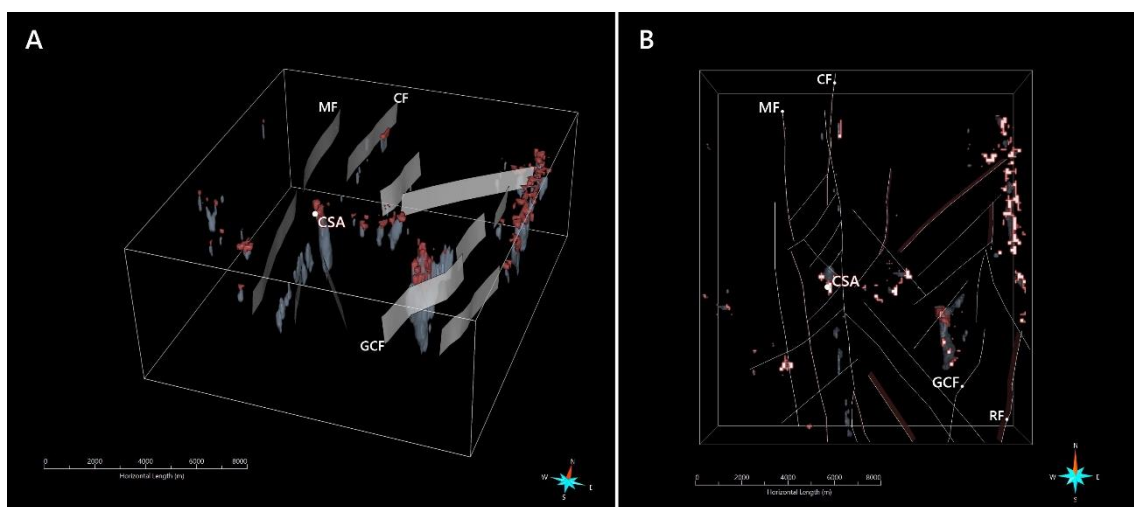

Figure 5. Magnetic bodies having susceptibility values ≥ 0.005 SI generated with VOXI MVI (red closed surfaces) and VOXI SUS (blue closed surfaces) across the CSA Mine region. Figure5A is a view from SE showing some major faults (white 3D surfaces); Figure 5B is a plan view showing the location of major faults (red 3D surfaces bordered by white lines). MF= Myrt Fault; CF= Cobar Fault; GCF= Great Chesney Fault; RF= Roockery Fault. The location of the inverted model is shown in Figure 1.

Peak Gold Mine Region Inverted 3D Model

The Peak Gold Mine deposit sits on a positive magnetic anomaly with intensity values up to 50nT (Figure 3). Within the Peak Gold Mine Region Inverted 3D Model, the host rock has a calculated magnetic susceptibility <0.001 SI (Figure 6). VOXI MVI results show that relatively magnetized, near-surface source bodies exhibit computed susceptibility values up to 0.036 SI (up to 0.0004 SI at the 90th percentile). Similar normal distribution of susceptibility values is observed for VOXI SUS (susceptibility values up to 0.0003 SI at the 90th percentile and a maximum value of 0.064 SI). Near-surface rocks with susceptibility values ≥ 0.005 SI appear to be predominantly located next to the NNE-trending Great Chesney Fault, at the junction with NNW to NW-trending faults (Figure 7). These magnetized rocks show vertical thickness ranging from 40m to ca 1300m. The lowest value depends on the model resolution.

The Great Cobar Mine is associated with a prominent magnetic anomaly, showing larger amplitude values compared to the anomalies associated with CSA and Peak Gold deposits (Figure 3). Both Peak Gold Mine and Great Cobar Mine correlate with relatively highly magnetic rocks with peak susceptibility values > 0.02 SI. Results from VOXI MVI and VOXI SUS are comparable for source bodies having susceptibility values ≥ 0.005 SI (Figure 7). Interestingly, the VOXI SUS identified magnetic rocks in correspondence to Chesney and New Cobar/Jubilee mines. Also, VOXI SUS show magnetized rocks in correspondence to Perseverance Mine, which is located about 800m below the topographic surface. The models indicate that the magnetic source-body at Perseverance Mine is part of a larger magnetic region that extends west of Peak Gold Mine and has NNW trend. VOXI MVI did not image magnetized rocks at Perseverance Mine but instead generated a distinct magnetized body to the immediate west of Peak Gold and Perseverance, situated ca 600m below the topographic surface.
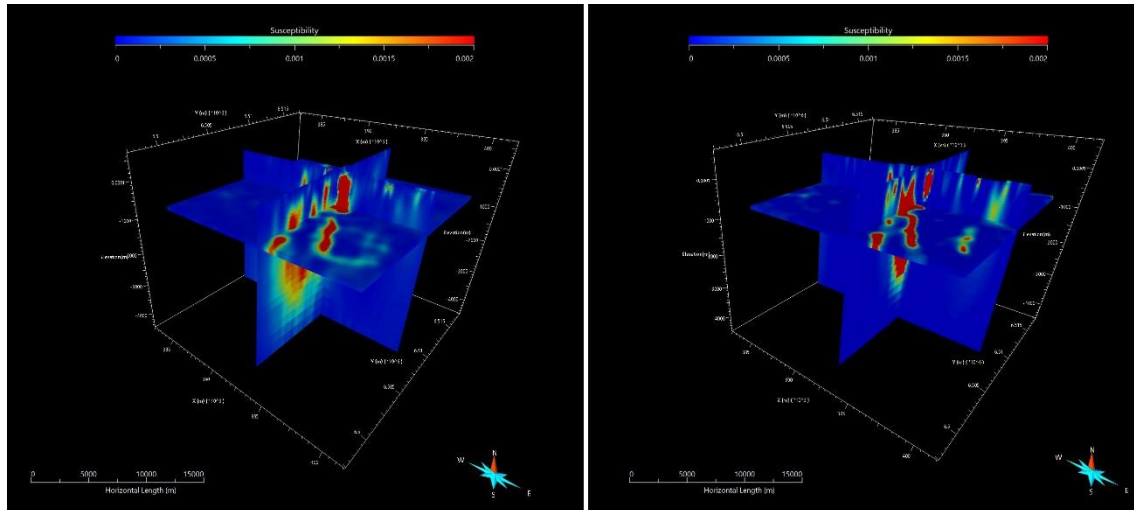
Figure 6. Results from VOXI MVI (A) and VOXI SUS (B) for the Peak Gold Mine region. Magnetic susceptibilities are in SI. The image has a 3X times vertical exaggeration. The location of the inversion model is shown in Figure 1.
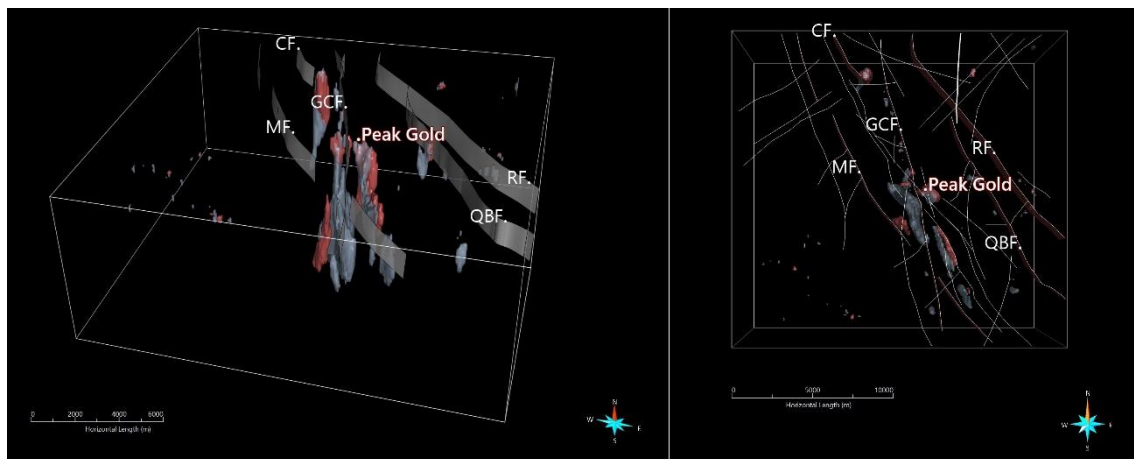

Figure 7. Magnetic bodies having susceptibility values ≥ 0.005 SI generated with VOXI MVI (red magnetic bodies) and VOXI SUS (blue magnetic bodies) across the Peak Gold Mine region. Figure 7A is a view from south showing some major faults (white 3D surfaces); Figure 7B is a plan view showing the location of major faults (red 3D surfaces bordered by white lines). MF= Myrt Fault; CF= Cobar Fault; GCF= Great Chesney Fault; RF= Roockery Fault; QBF= Queen Bee Fault. The location of the inverted model is shown in Figure 1.

Hera Mine Region Inverted 3D Model

In the Hera Mine region, VOXI MVI and VOXI SUS show that the host rock has a calculated magnetic susceptibility below 0.001 SI. In the south-western and north-eastern part of the inverted 3D model, weakly to moderately magnetized source bodies with susceptibility values up to 0.006 SI are imaged at a depth > 2km (Figure 8). VOXI MVI generated shallow magnetized rocks with susceptibility values ≥ 0.004 SI that appear to sit on or next to major NNW-trending structures including the Roockery Fault and at the hinge of regional culminations. The Hera Mine is located on the western side of the Rookery Fault.

The Nymagee deposit is located to the immediate north of the Hera deposit, on the western side of the Rookery Fault and corresponds to a prominent magnetic anomaly (see next section), while rocks associated with the Hera Mine do not show discernible magnetic signature. South of Hera, VOXI MVI produced a magnetized, steeply dipping lens with a thickness up to ca 275m (for susceptibility values ≥0.004 SI) corresponding to the South Peak Prospect (Figure 9). Magnetic domains have also been generated east of the Ironbark Fault, at the intersection between NNW-trending and NE-trending faults (Figure 9). VOXI SUS produced co-located but considerably thicker magnetic regions extending up to ca 920m depth.
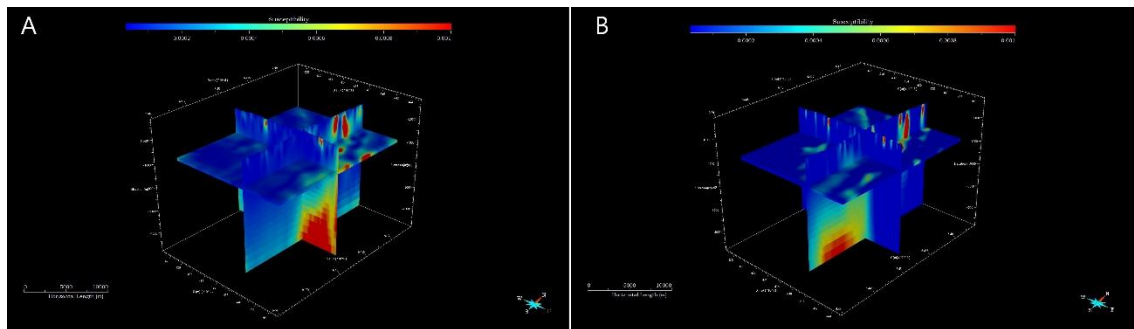
Figure 8. Results from the VOXI MVI (A) and VOXI SUS (B) for the Hera and Nymagee region. Magnetic susceptibilities are in SI. The image has a 3X times vertical exaggeration. The location of the inversion model is shown in Figure 1.

A major discrepancy in the inversion results occurs at Nymagee Mine. The magnetic region generated by VOXI SUS is significantly smaller if compared to the magnetized volume computed by VOXI MVI.

Within the modelled region, purely induced inversion performed with both VOXI SUS produced additional magnetized source bodies smaller in size and located next to the major NNW-trending structures.
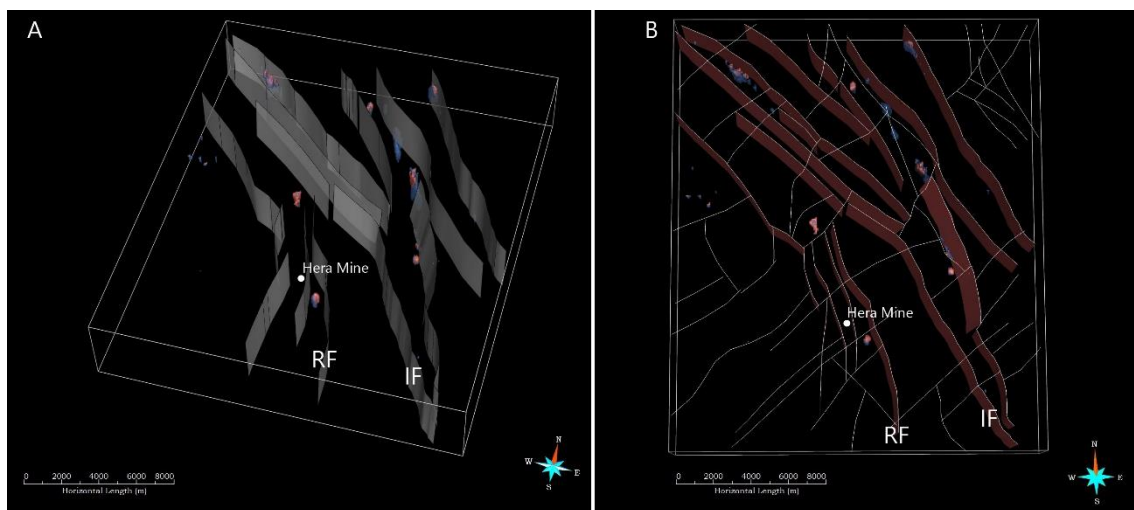

Figure 9. Magnetic bodies having susceptibility values ≥ 0.004 SI generated with VOXI MVI (red magnetic bodies) and VOXI SUS (blue magnetic bodies). Figure 9A is a view from SSE showing major NW-trending faults (white 3D surfaces); Figure 9B is a plan view showing the location of major faults (red 3D surfaces bordered by white line) and minor structures (white lines). RF= Roockery Fault; IF= Ironbark Fault. The image has a 3X times vertical exaggeration. The location of the inversion model is shown in Figure 1.

South Cobar Region Inverted 3D Model

The South Cobar Region Inverted 3D Model is characterized by significant lateral variation in the calculated magnetic susceptibility of both near-surface and deeper rocks. VOXI MVI generated magnetic source bodies, with susceptibility values comprised between 0.002 SI and 0.009 SI, extending all the way from the bottom of the model to shallow depth in vein-like configuration (Figure 10). VOXI SUS also highlighted magnetized rocks in pipe-like disposition, although the distribution of the susceptibility values tends to diverge for depth >1500m between the models (Figure 11). Source bodies produced with VOXI MVI with a calculated magnetic susceptibility ≥ 0.005 are shown in Figure 10. The source bodies appear to be located in shear zones and at the junction of major N-S- to NNE-trending faults, including the Kilparney and Woorara faults, and NE- to NW-trending tear faults. The computed vertical thickness of these magnetized rocks is in the range of a few hundreds of meters. In the south-eastern part of the area of interest, the produced magnetic source bodies show vertical thickness >1500m (Figure 10 and Figure 11). The distribution of near-surface magnetic rocks generated with magnetic vector inversion and purely induced susceptibility inversion are comparable, although the vertical extension and shape of co-located source bodies show some variation from one inversion method to another. VOXI SUS generated scattered and relatively small magnetic domains that are not produced in the VOXI MVI model (Figure 11). Both inversion methods resulted in co-located, elongated source bodies showing slightly divergent dip angle and dip direction. The geometrical variation is more apparent in the north-western and south-eastern parts of the area of interest (Figure 11).
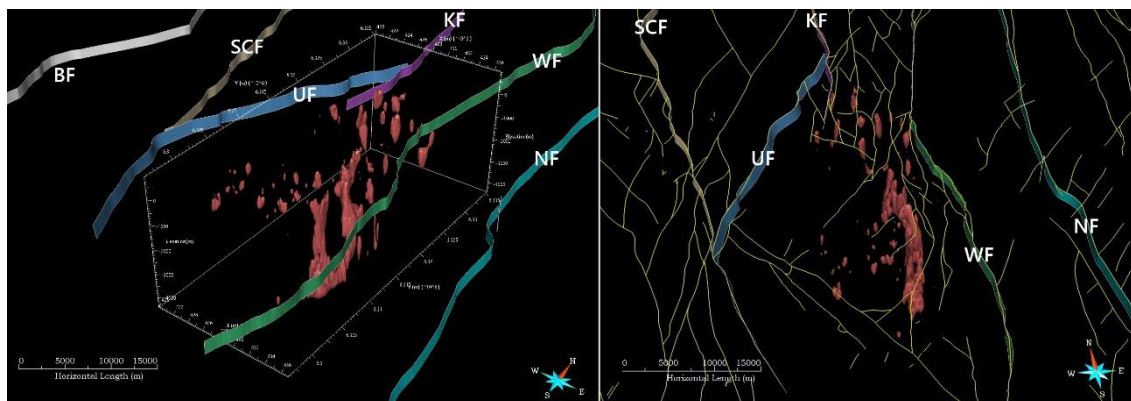
Figure 10. Magnetic bodies having susceptibility values ≥ 0.005 SI generated with VOXI MVI across the south Cobar region. To the left, view from SE (3X times vertical exaggeration); to the right, plant view. BF= Bootheragandra Fault; SCF= Scotts Craig Fault; UB= Uabba Fault; KF= Kylparney Fault; WF= Woorara Fault; NF= Narriah Fault. The location of the inverted model is shown in Figure 1.
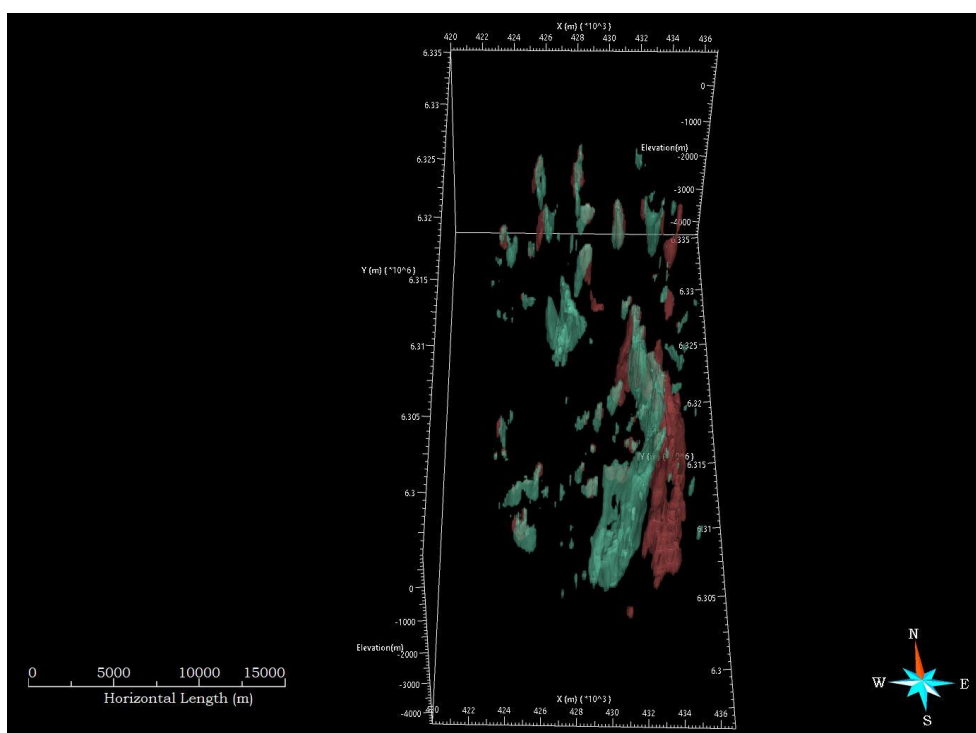

Figure 11. Magnetic bodies with susceptibilities ≥ 0.005 generated with VOXI MVI (red envelopes) and VOXI SUS (green envelopes) across the south Cobar region. The image has a 3X times vertical exaggeration. The location of the inversion model is shown in Figure 1.

DISCUSSION

Although lithological control through permeability, reactivity or competency contrast plays an important part during the mineralisation process (Fitzherbert et al., 2021), the inversion results indicate the location of mineral deposits is controlled by the basement architecture, supporting early observations by Glen (1987, 1995).

Known mineral deposits and prospective rocks occur near major structures and at the intersection or junction between inverted normal faults, thrust and strike-slip faults. This suggests that the major faults acted as pathways for enriched fluids. Tear faults intercepted these mineralised and metal enriched fluids in dilational sites at their intersection with other structures. The modelled magnetic source bodies might reflect disseminated pyrrhotite and magnetite associated with the Cobar-type deposits.

The two inversion algorithms (VOXI MVI and VOXI SUS) generated shallow magnetic bodies associated with high-wavelength magnetic anomalies. The outcomes from magnetic vector inversion and purely induced susceptibility inversion are comparable, but discrepancies exist in the lateral extension and thickness of the deposits generated by the two inversion methods.

The inversion results suggest that the mineralised rocks at the CSA Mine correlate with an elongated, weakly to moderately magnetic domain. However, peak magnetic intensity and thus calculated susceptibility values seem to be located under some infrastructures. Therefore, it is likely that the peak magnetic signal does not correspond to a geological feature, but it is rather an artifact due to anthropic activity. VOXI MVI indicates that the magnetised body related to the known deposit stretches a few hundred meters south of the magnetic high imaged in the RTP grid extending into a very low magnetic zone, implying that remanence could be a contributing factor to the net in situ magnetization.

The magnetic anomalies at Nymagee Mine might reflect the distribution of pyrrhotite, which occurs in both massive and disseminated forms and magnetite (Page, 2011). Mineralisation at Hera is characterized by non-magnetic pyrrhotite which reflect the high temperature skarn mineralogy (Fitzherbert et al., 2021) and thus does not display a notable magnetic signature. No co-located magnetized bodies have been generated by the two inversion methods.

An interesting case study is at Nymagee Mine (Figure 11). The TMI and RTP anomaly at the Nymagee deposit is dipolar and consists of positive intensity values to the north and a magnetic trough to the south (Figure 12). The known mineral occurrences are located at the magnetic peak (Figure 12). VOXI SUS generated a magnetic body located at the peak amplitude values (Figure 11). VOXI MVI inversion suggest instead that the total magnetisation amplitude and direction significantly differ from that of the inducing field. The causative body has a strong magnetization component and extends further north (Figure 11). In this scenario, half of the deposits sits under the magnetic low.
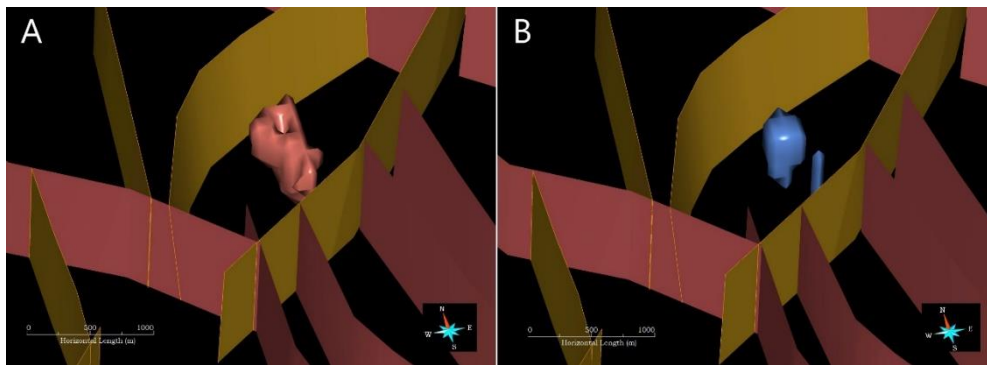

Figure 11. Inversion results at Nymagee Mine with VOXI MVI (A) and VOXI SUS (B).

Analysis of the analytic signal of aeromagnetic anomalies over the Nymagee deposit can be a complementary approach to the remanence issue. The resultant magnetisation for a given anomaly is the vector sum of the induced and remanent components (Ellis, 2012). The total magnetic intensity (TMI) and the reduction to the pole (RTP) maps of the aeromagnetic anomalies are sensitive to the magnetization direction. Therefore, RTP transform over the total magnetic anomalies only assuming induced magnetisation can potentially lead to odd resulting grids and errors in the interpretation phase if the direction of magnetization of the causative bodies is not known (Rajagopalan, 2003). On the other hand, the analytic signal (AS) of the aeromagnetic anomalies is a function of magnetic gradients and it is less sensitive to the ambient magnetic field and source magnetization direction, thus reducing the effects of remanent magnetization (Linping et al., 1997; Qin, 1994; Rajagopalan, 2003; Roest and Pilkington, 1993). As a result, the analytic signal exhibits maxima over magnetization contrasts, that will help determining the outlines of magnetic source (Roest et al., 1992). At Nymagee Mine, the AS grid shows a single high that includes the magnetic peak (where known mineralization occurs) and magnetic low imaged in the RTP grid (Figure 12). The discrepancies between the RTP and the AS grids suggest that remanent magnetization could be determinant component of the net in situ magnetization.
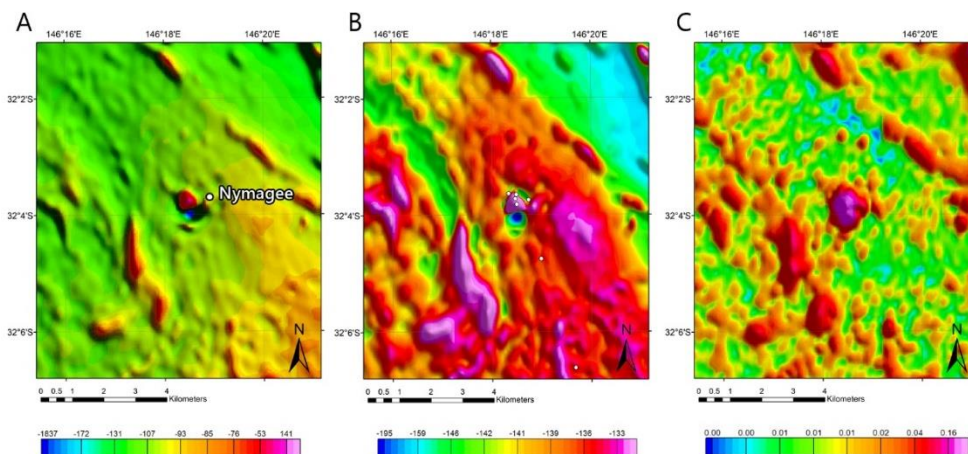
Figure 12. Pseudo-colour image of the TMI (A) and RTP (B) and AS (C) of aeromagnetic anomalies over the Nymagee deposit. White points are known mineral occurrences.

In the south Cobar district, inversion results indicate the N-S-trending structural corridor comprised between the Kilparney and Woorara faults have potential to host mineralisation. The significant heterogeneity in the calculated susceptibility values might reflect diffuse presence of magnetite and pyrrhotite rich rocks within the host units. Discrepancies in extent and geometries of the magnetized domains generated by the two inversion methods tends to be more pronounced in the southern part of the modelled area. This also has implication on the estimated volumes of the prospective rocks and suggests that remanent magnetization is a component of the magnetic signature of these deposits. These results support the findings from Clark and Tonkin (1992) who suggest that the remanence is the dominant contributor to the magnetisation across the region.

CONCLUSIONS

Aeromagnetic data and 3D EM inversion indicate that major N-S- to NNW-trending faults control basin architecture and the location of the known mineral occurrences and prospective rocks at the regional scale. At the camp scale, magnetized source bodies are localised within high strain zones and at the intersection of the major N-S- to NNW-trending structures and NE- to NW-trending strike-slip faults.
Major faults along with lithological contacts might have acted as pathways for fluid flow. Dilation zone focussed ore-fluid flux and subsequent mineral deposition.

This research support previous studies but most importantly establishes a methodology to discover the next deposit undercover through an integrated approach in 3D geological modelling and 3D geophysical inversion. The unconstrained 3D inversion not only highlighted source bodies associated to the CSA, Peak Gold and Nymagee deposits but also identified prospective rocks of the Cobar mineral system that are underexplored.
The discrepancies in the outcome of magnetic vector inversion and purely induced susceptibility inversion, along with analysis of the magnetic signal suggest that remanent magnetization is a significant component of the magnetic signature of the Cobar deposits.

Potential mineralised terranes undercover in the Cobar district might only be under a few 10s m of cover material and might be economically viable.

ACKNOWLEDGMENTS

REFERENCES

Aillères, L., 2000. New gOcad® developments in the field of 3-dimensional structural geophysics. J. Virtual Explor. 1. https://doi.org/10.3809/jvirtex.2001.0006

Betts, P.G., Giles, D., Lister, G.S., 2004. Aeromagnetic patterns of half-graben and basin inversion: Implications for sediment-hosted massive sulfide Pb-Zn-Ag exploration. J. Struct. Geol. 26, 1137–1156.

Clark, D.A., Tonkin, C., 1994. Magnetic anomalies due to pyrrhotite: examples from the Cobar area, N.S.W., Australia. J. Appl. Geophys. 32. https://doi.org/10.1016/0926-9851(94)90006-X

Colquhoun, G.P., Hughes, K.S., Deyssing, L., Ballard, J.C., Phillips, G., Troedson, A.L., Folkes, C.B., Fitzherbert, J.A., 2020. New South Wales Seamless Geology dataset, version 2.0 [Digital Dataset]. Geological Survey of New South Wales, Department of Regional NSW, Maitland.

David, V., 2018. Cobar Deposits - Structural control. ASEG Ext. Abstr. 2018.

Elllis, R.G., de Wet, B., Macleod, I.N., 2012. Inversion of Magnetic Data from Remanent and Induced Sources. ASEG Ext. Abstr. 2012. https://doi.org/10.1071/aseg2012ab117

Fitzherbert, J., 2020. A mineral system model for Cu-Au-Pb-Zn-Ag systems of the Cobar Basin, central Lachlan Orogen, New South Wales A mineral system model for Cu-Au-Pb-Zn-Ag systems of the Cobar Basin, central Lachlan Orogen, New South Wales Title: A mineral system model for.

Fitzherbert, J.A., McKinnon, A.R., Blevin, P.L., Waltenberg, K., Downes, P.M., Wall, C., Matchan, E., Huang, H., 2021. The Hera orebody: A complex distal (Au–Zn–Pb–Ag–Cu) skarn in the Cobar Basin of central New South Wales, Australia. Resour. Geol. 71. https://doi.org/10.1111/rge.12262

Folkes, C.B., Carlton, A., Eastlake, M., Deyssing, L., Trigg, S., Montgomery, K., Matthews, S., Spampinato, G., Roach, I, Ley-Cooper, Y., Wong, S., 2021. The Cobar AEM interpretation report. Geol. Surv. New South Wales, Rep. GS2021/1645.

Fullagar, P.K., Pears, G.., 2013. The need for geological and petrophysical constraints in geophysical inversion. Invers. forum.

Glen, R.A., 1995. Thrusts and thrust-associated mineralization in the Lachlan Orogen. Econ. Geol. 90, 1402–1429. https://doi.org/10.2113/gsecongeo.90.6.1402

Glen, R.A., 1991. Inverted transtensional basin setting for gold and copper and base metal deposits at Cobar, New South Wales. BMR J. Aust. Geol. Geophys. 12.

Glen, R.A., 1987. Copper- and gold-rich deposits in deformed turbidites at Cobar, Australia: their structural control and hydrothermal origin. Econ. Geol. https://doi.org/10.2113/gsecongeo.82.1.124

Linping, H., Zhining, G., Changli, Y., 1997. Comment on: "an analytic signal approach to the interpretation of total field magnetic anomalies" by Shuang Qin. Geophys. Prospect. 45.

Page, D.G., 2011. Geology of the Hera (Pb-Zn-Au) and Nymagee (Cu) deposits, New South Wales. University of Wollongong, School of Earth and Environmental Sciences, Bachelor of Science (Honours), Thesis, 212p.

Qin, S., 1994. An analytic signal approach to the interpretation of total field magnetic anomalies. Geophys. Prospect. 42. https://doi.org/10.1111/j.1365-2478.1994.tb00234.x

Rajagopalan, S., 2003. Analytic signal vs. reduction to pole: Solutions for low magnetic latitudes. Explor. Geophys. 34. https://doi.org/10.1071/EG03257

Roest, W.R., Pilkington, M., 1993. Identifying Remanent Magnetization Effects in Magnetic Data. Geophysics 58, 653–659. https://doi.org/10.1190/1.1443449

Roest, W.R., Verhoef, J., Pilkington, M., 1992. Magnetic interpretation using the 3-D analytic signal. GEOPHYSICS 57. https://doi.org/10.1190/1.1443174

Spampinato, G.P.T., 2022. 3D modelling of the AEM survey interpretation for the North and South Cobar National Drilling Initiative areas.

Spampinato, G.P.T., Ailleres, L., Betts, P.G., Armit, R.J., 2015a. Imaging the basement architecture across the Cork Fault in Queensland using magnetic and gravity data. Precambrian Res. 264. https://doi.org/10.1016/j.precamres.2015.04.002

Spampinato, G.P.T., Betts, P.G., Ailleres, L., Armit, R.J., 2015b. Structural architecture of the southern Mount Isa terrane in Queensland inferred from magnetic and gravity data. Precambrian Res. 269. https://doi.org/10.1016/j.precamres.2015.08.017

Williams, H.A., Betts, P.G., Ailleres, L., Burtt, A., 2010. Characterization of a proposed Palaeoproterozoic suture in the crust beneath the Curnamona Province, Australia. Tectonophysics. https://doi.org/10.1016/j.tecto.2009.12.008

Witter, J.B., 2015. GOCAD ® Mining Suite Software as a Tool for Improved Geothermal Exploration, in: World Geothermal Congress 2015. p. 5.

Witter, J.B., Siler, D.L., Faulds, J.E., Hinz, N.H., 2016. 3D geophysical inversion modeling of gravity data to test the 3D geologic model of the Bradys geothermal area, Nevada, USA. Geotherm. Energy 4.